

# Electric field control of Jahn-Teller distortions in bulk perovskites

Julien Varignon,<sup>1,\*</sup> Nicholas C. Bristowe,<sup>1,2,\*</sup> and Philippe Ghosez<sup>1</sup>

<sup>1</sup>*Physique Théorique des Matériaux, Université de Liège (B5), B-4000 Liège, Belgium*

<sup>2</sup>*Department of Materials, Imperial College London, London SW7 2AZ, UK*

(Dated: May 14, 2015)

The Jahn-Teller distortion, by its very nature, is often at the heart of the various electronic properties displayed by perovskites and related materials. Despite the Jahn-Teller mode being non-polar in nature, we devise and demonstrate in the present letter an electric field control of Jahn-Teller distortions in bulk perovskites. The electric field control is enabled through an anharmonic lattice mode coupling between the Jahn-Teller distortion and a polar mode. We confirm this coupling, and explicitly an electric field effect, through first principles calculations. The coupling will always exist within the  $Pb2_1m$  space group, which is found to be the favoured ground state for various perovskites under sufficient tensile epitaxial strain. Intriguingly, the calculations reveal that this mechanism is not only restricted to Jahn-Teller active systems, promising a general route to tune or induce novel electronic functionality in perovskites as a whole.

Perovskites, and related materials, are fascinating systems exhibiting a diverse collection of properties, including ferroelectricity, magnetism, orbital-ordering, metal-insulator phase transitions, superconductivity and thermoelectricity<sup>1</sup>. Despite the wide range of physical behaviour, a common point at the origin of many of them can be identified as being the Jahn-Teller distortion<sup>2,3</sup>. The Jahn-Teller distortion is itself intimately linked to electronic degrees of freedom, since traditionally it manifests to remove an electronic degeneracy, opening a band gap and favouring a particular orbital ordering, which in turn can affect magnetic ordering. Furthermore it plays an important role, for example, in colossal magnetoresistance phenomena in doped manganites<sup>4</sup>, superconductivity<sup>5,6</sup> or the strong electronic correlation observed in the thermoelectric NaCoO<sub>2</sub> family<sup>7</sup>.

It would be highly desirable, for device functionality for example, to be able to tune the Jahn-Teller distortion and hence its corresponding electronic properties, with the application of an external electric field. However, Jahn-Teller distortions are non-polar and hence not directly tunable with an electric field. One strategy to achieve an electric field control of Jahn-Teller distortions might begin by engineering a polar structure. Usually, perovskites adopt a non-polar  $Pbnm$  ground state, resulting in a combination of three rotations of the oxygen octahedra ( $a^-a^-c^+$  in Glazer's notation<sup>8</sup>), also called antiferrodistortive (AFD) motions. Unfortunately, these AFD distortions are known to often prevent<sup>9</sup> the appearance of the polarization in the material. The use of anharmonic lattice mode couplings between polar and non-polar lattice distortions is a promising pathway to engineer "improper" ferroelectricity in layered perovskite derivatives<sup>10-13</sup>, and furthermore to achieve novel functional possibilities via these couplings<sup>14-20</sup>. Interesting anharmonic couplings do not only exist in layered perovskites, but can also appear in bulk ABO<sub>3</sub> perovskites<sup>19,21,22,25-28</sup>

Following this spirit, achieving an electric field control of Jahn-Teller distortions necessarily requires the identification of a material exhibiting a relevant coupling be-

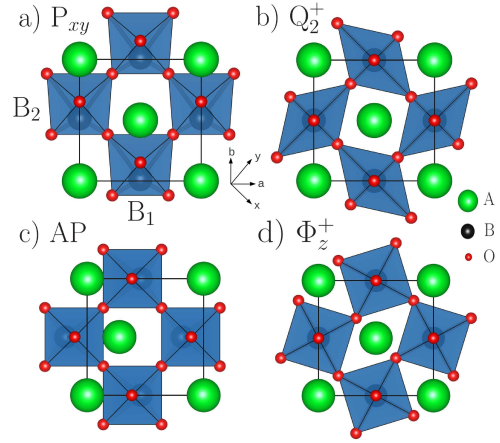


FIG. 1. Schematic view of the four lattice distortions involved in the  $Pb2_1m$  phase of perovskites under tensile epitaxial strain. a) Polar distortion (irreps  $\Gamma_5^-$ ) b)  $Q_2^+$  Jahn-Teller distortion (irreps  $M_3^+$ ) c) Anti-polar A distortion (irreps  $M_5^+$ ) d)  $a^0a^0c^+$   $\phi_z^+$  antiferrodistortive motion (irreps  $M_2^+$ ).

tween the polarization and the Jahn-Teller distortion, which to the best of our knowledge has not yet been discovered in bulk perovskites<sup>23</sup>. In the present letter we identify such conditions, and demonstrate explicitly an electric field control, in bulk perovskites using a combination of symmetry analysis and first principles calculations.

## RESULTS

The two required lattice distortions are pictured in figure 1. a) and b). From a symmetry analysis of the different tilt patterns in combination with possible Jahn-Teller lattice distortions, Howard and Carpenter pointed out that a Jahn-Teller distortion pattern automatically appears when considering the  $Pbnm$  symmetry<sup>25</sup>, later

explained in terms of anharmonic couplings with AFD motions<sup>19</sup>. As a consequence, a Jahn-Teller distortion is not necessarily electronically driven, but can instead arise from lattice mode couplings in which case a splitting of the electronic states may develop even in the absence of a degeneracy of states. The present Jahn-Teller lattice motion corresponds to a  $Q_2$  mode as defined by Goode-nough<sup>3</sup>, corresponding to two B-O bond length contractions and two B-O elongations. This motion orders at the M point of the Brillouin zone and hence consecutive layers along the  $\vec{c}$  axis of the  $Pbnm$  phase present in-phase distortions. Consequently, this motion is labelled  $Q_2^+$  (irreps  $M_3^+$ ) throughout the whole manuscript.

Starting from the ideal  $Pm\bar{3}m$  cubic perovskite phase, the condensation of the polar mode P (irreps  $\Gamma_5^-$ ) and the JT mode  $Q_2^+$  lowers the symmetry to a  $Pb2_1m$  phase, a polar subgroup of  $Pbnm$ . We then perform a free energy expansion<sup>29</sup> in terms of the possible lattice distortions in this new phase and we identify, among all the possible terms, some intriguing couplings:

$$\mathcal{F} \propto PQ_2^+A + P^2Q_2^+\phi_z^+ + P\phi_z^+A + Q_2^+\phi_z^+A^2 \quad (1)$$

In this phase, the first two terms of equation 1 provide a link between the polarization and the Jahn-Teller distortion. These terms also involve two additional distortions: one anti-polar A motion pictured in figure 1. c) and one  $a^0a^0c^+$  AFD motion (labelled  $\phi_z^+$ ) pictured in figure 1. d). Among all the terms, the lowest order trilinear term of the form  $PQ_2^+A$  provides the desired direct coupling between the polarization and the JT distortion. Thus, acting on the polarization with an external electric field may modify the amplitude of the JT motion, and therefore all related electronic properties.

However, as previously discussed, the  $Pb2_1m$  symmetry is not the common ground state in bulk perovskites<sup>24</sup>. Strain engineering, through thin film epitaxy for example, can provide a powerful tool to unlock a polar mode in perovskites<sup>13,30-35</sup>. This is the case for BiFeO<sub>3</sub> that was recently proposed to adopt an unusual  $Pb2_1m$  symmetry under large epitaxial tensile strain<sup>26,27,36</sup>. This particular phase was shown to develop both polar, anti-polar and  $a^0a^0c^+$  AFD motions<sup>26</sup>, which were later demonstrated to be coupled together through the third term of eq. 1<sup>27</sup>. Amazingly, the authors reported the existence of an orbital ordering of the Fe<sup>3+</sup> 3d orbitals, explained from the coexistence of the polar and the anti-polar motion yielding a particular lattice distortion pattern<sup>26</sup>. This orbital-ordering is unusual since in this system no Jahn-Teller effect is required to form a Mott insulating state (Fe<sup>3+</sup> are in a half filled - high spin  $t_{2g}^3e_g^2$  configuration). A Jahn-Teller effect or distortion are yet to be reported in the  $Pb2_1m$  phase of BiFeO<sub>3</sub> to the best of our knowledge. From our symmetry analysis, we clearly demonstrate that as this  $Pb2_1m$  develops the three aforementioned distortions (P, A and  $\phi_z^+$ ), the free energy of eq. 1 is automatically lowered through the appearance of a fourth lattice distortion: a Jahn-Teller  $Q_2^+$  motion. Therefore, whilst it may not itself be unstable, the Jahn-Teller mo-

tion is forced into the system via this “improper” mechanism arising from the trilinear coupling<sup>10</sup>. This result clarifies the origin of the unusual orbital-ordering displayed by BiFeO<sub>3</sub> and moreover, it provides a pathway to achieve an electric field control of the orbital-ordering in bulk perovskites.

The predicted highly strained  $Pb2_1m$  phase in bulk perovskites is not restricted to BiFeO<sub>3</sub>, and it was predicted to occur also in some titanates (CaTiO<sub>3</sub> and EuTiO<sub>3</sub>)<sup>26</sup>, in BaMnO<sub>3</sub><sup>26</sup> and even in a Jahn-Teller active compound TbMnO<sub>3</sub><sup>37</sup>. The highly strained bulk perovskites are then an ideal playground to demonstrate our coupling between the polarization and the Jahn-Teller distortion. In order to check the generality of our concept, we propose in this letter to investigate several types of highly strained perovskites on the basis of first principles calculations: i) non magnetic (NM) SrTiO<sub>3</sub> ( $t_{2g}^0e_g^0$ ); ii) magnetic BaMnO<sub>3</sub><sup>38</sup> ( $t_{2g}^3e_g^0$ ) and BiFeO<sub>3</sub> ( $t_{2g}^3e_g^2$ ); iii) Jahn-Teller active YMnO<sub>3</sub> ( $t_{2g}^3e_g^1$ ).

We begin by investigating the possibility of a  $Pb2_1m$  ground state under large epitaxial tensile strain (the growth direction is along the [001] axis of the  $Pbnm$  structure). Beyond around 5% tensile strain, the four compounds indeed develop the desired  $Pb2_1m$  ground state. Strained BaMnO<sub>3</sub> (ferromagnetic FM) and YMnO<sub>3</sub> (G-type antiferromagnetic AFMG) exhibit a different magnetic ground state compared to the bulk (AFMG and E-type antiferromagnetic -  $\uparrow\uparrow\downarrow\downarrow$  zig-zag chains coupled antiferromagnetically along the  $\vec{c}$  axis - respectively) while BiFeO<sub>3</sub> (G-type antiferromagnetic AFMG) remains in its bulk magnetic ground state. We then perform a symmetry mode analysis with respect to a hypothetical  $P4/mmm$  phase (corresponding to  $Pm\bar{3}m$  for unstrained bulk compounds) in order to extract the amplitude of the relevant lattice distortions<sup>40</sup> (see table I). As expected, the four materials develop the required distortions, and amazingly, the magnitude of the  $Q_2^+$  Jahn-Teller distortion is relatively large, being for instance of the same order of magnitude as the one developed in the prototypical Jahn-Teller system LaMnO<sub>3</sub> (around 0.265 Å<sup>41</sup>). Additionally, the values of the spontaneous polarization are rather large, reaching 76

		SrTiO <sub>3</sub>	BaMnO <sub>3</sub>	BiFeO <sub>3</sub>	YMnO <sub>3</sub>
strain	(%)	+7.35 <sup>39</sup>	+6.1 <sup>39</sup>	+5.8 <sup>39</sup>	+4.0 <sup>39</sup>
magnetism		NM	FM	AFMG	AFMG
P ( $\Gamma_5^-$ )	(Å)	0.615	0.421	0.346	0.753
	( $\mu C.cm^{-2}$ )	76	45	29	7 <sup>7</sup>
$Q_2^+$ ( $M_3^+$ )	(Å)	0.232	0.190	0.644	0.737
A ( $M_5^+$ )	(Å)	0.558	0.217	1.072	0.940
$\phi_z^+$ ( $M_2^+$ )	(Å)	0.640	0.059	1.668	1.733
gap	(eV)	3.02	0.28	1.88	1.88

TABLE I. Epitaxial strain (%), magnetic ground state, amplitudes of distortions (Å) and electronic band gap value (eV) for each material. We emphasize that only the relevant distortions are summarized in the present table.

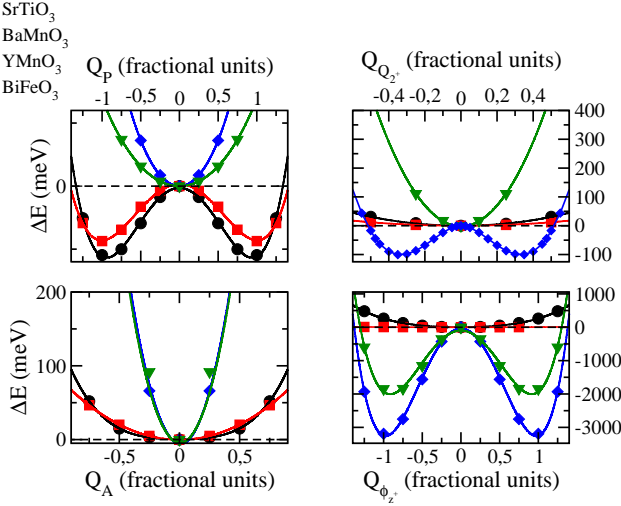


FIG. 2. Potentials with respect to the amplitude of distortions of the four lattice motions producing the required  $Pb2_1m$  for SrTiO<sub>3</sub> (black filled circles), BaMnO<sub>3</sub> (red filled squares), YMnO<sub>3</sub> (blue filled diamonds) and BiFeO<sub>3</sub> (green filled triangles) starting from the ideal  $P4/mmm$  phase.

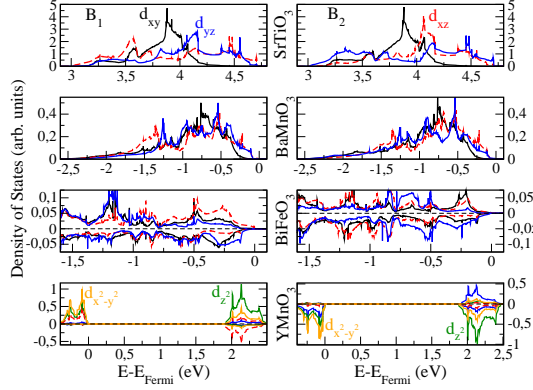


FIG. 3. Projected density of states on the  $d$  levels on two neighboring B sites in the  $(ab)$ -plane of SrTiO<sub>3</sub>, BaMnO<sub>3</sub>, BiFeO<sub>3</sub> and YMnO<sub>3</sub>. Local axes of the orbitals are displayed on figure 1. The Fermi level is located at 0 eV.

$\mu C.cm^{-2}$  for SrTiO<sub>3</sub> for instance. Despite being highly strained, all materials remain insulating, adopting reasonable electronic band gap values (see table I).

To shed more lights on the origin of this unusual  $Pb2_1m$  phase we compute the energy potentials with respect to the four distortions by condensing individually each modes in an hypothetical  $P4/mmm$  phase (see figure 2). Surprisingly, the appearance of the  $Pb2_1m$  phase is rather different for the four materials. SrTiO<sub>3</sub> and BaMnO<sub>3</sub> only exhibit a polar instability, producing an  $Amm2$  symmetry, consistent with previous reports of a polar phase for these two materials under tensile strain<sup>30,42</sup>. Computing the phonons in this particular  $Amm2$  symmetry, only one hybrid unstable phonon mode is identified for these two materials, having a mixed char-

acter between the A,  $\phi_z^+$  and  $Q_2^+$  distortions, For BiFeO<sub>3</sub> and YMnO<sub>3</sub>, the  $a^0a^0c^+$  AFD motion is already unstable, which is expected since the  $Pb2_1m$  symmetry for these two systems is derived from their bulk  $R3c/Pbnm$  phases<sup>40</sup>. Additionally, the JT lattice distortion is also unstable in the  $P4/mmm$  phase of YMnO<sub>3</sub> and appears as an electronic instability<sup>43</sup>, which is expected since YMnO<sub>3</sub> is known to be Jahn-Teller active in the bulk. We emphasize at this stage that the polar mode in BiFeO<sub>3</sub> (and YMnO<sub>3</sub>) is not unstable and therefore highly strained BiFeO<sub>3</sub> appears as an improper ferroelectric in contradiction to reference 27. Computing the phonons in the intermediate strained  $Pbnm$  phase of both BiFeO<sub>3</sub> and YMnO<sub>3</sub> compounds reveals only one hybrid unstable mode, having a mixed character between P and A distortions. Despite the apparent universal stability of this highly strained polar phase, the mechanism yielding it is surprisingly different between the compounds.

Regarding the electronic structure, we checked for the appearance of an orbital ordering as observed in BiFeO<sub>3</sub><sup>26</sup>. For the four compounds we report the projected density of states on the  $d$  levels of two neighboring B sites in the  $(ab)$ -plane (see figure 3). For SrTiO<sub>3</sub>, a splitting of the  $t_{2g}$  states, and especially between the  $d_{xz}$  and  $d_{yz}$  orbitals, located at the bottom of the conduction band arises. For BaMnO<sub>3</sub> and BiFeO<sub>3</sub>, a similar splitting between the  $t_{2g}$  levels is observed near the Fermi level, even if it is less pronounced for BaMnO<sub>3</sub> since it has the smallest  $Q_2^+$  distortion. Finally, YMnO<sub>3</sub> displays an orbital ordering of the  $e_g$  levels with predominantly  $d_{x^2-y^2}$  occupation. This splitting is known to result of the Jahn-Teller distortion in this  $A^{3+}Mn^{3+}O_3$  class of material<sup>45</sup>. Additionally, an orbital ordering of the  $t_{2g}$  levels is occurring both in the conduction and the valence bands. To prove that the Jahn-Teller distortion, and not another motion, is solely responsible for the orbital ordering we have condensed all the modes individually and studied the density of states (see supplementary figure 1).

Finally, we explicitly demonstrate the electric field control of Jahn-Teller distortion by computing, as a function of the electric field  $\vec{E}$  applied along the direction of the spontaneous polarization, the evolution of both the JT distortion and the band gap. Results are displayed in figure 4. The Jahn-Teller distortion is effectively altered by the application of an electric field along the polar axis through the first and second terms of equation 1. As the electric field increases, the amplitude of the JT distortion is either amplified or decreased, being renormalized to around 175% for SrTiO<sub>3</sub> for an electric field around 20 MV.cm<sup>-1</sup>. The largest effect is however reached for YMnO<sub>3</sub> which displays a renormalization of 130% under moderate electric field (around 5 MV.cm<sup>-1</sup>). Therefore, this renormalization of the JT distortion has consequences for instance on the electronic band gap value, with an opening/closure around 0.6 eV for YMnO<sub>3</sub> or 0.25 eV for SrTiO<sub>3</sub>. It is then possible, through the coupling between the polarization and the Jahn-Teller distortion to act on the electronic band gap, and one

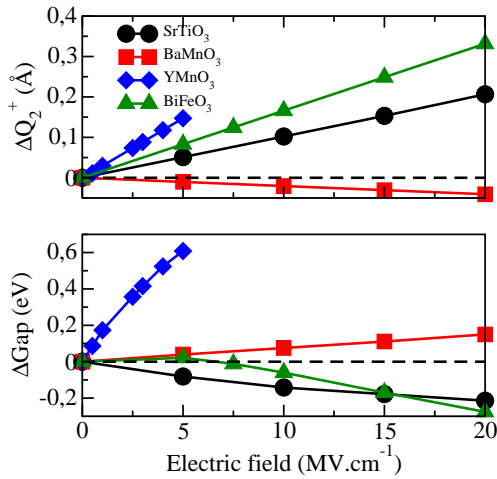


FIG. 4. Relative electric field effect on the amplitude of the Jahn-Teller distortion (top panel) and the electronic gap value (bottom panel) on the four different compound.

may imagine a possible control of a Metal-Insulator phase transition, optical properties, or photovoltaic efficiency, for instance.

In conclusion, we have demonstrated in the highly strained  $Pb2_1m$  phase of bulk perovskites the existence of a coupling between a polar mode and the Jahn-Teller distortion. This improper anharmonic coupling, established on universal symmetry arguments, enables an electric field control of the Jahn-Teller distortion, even in the case of non electronically Jahn-Teller active systems. The generic mechanism may open novel functionalities in perovskites as it will have consequences on related electronic properties as proposed in the present letter. For instance, such couplings may allow the tuning of Metal-Insulator phase transitions, the control of orbital orderings, optical properties, or of the photovoltaic efficiency.

## METHODS

First-principles calculations were performed with the VASP package<sup>47,48</sup>. We used the PBEsol<sup>49</sup>+U framework as implemented by Lichtenstein's method<sup>50</sup> (see the supplementary material for a discussion on the choice of the U and J parameters). The plane wave cut-off was set to 500 eV and we used a  $6 \times 6 \times 4$  k-point mesh for the 20 atom  $Pb2_1m$  phase. PAW pseudopotentials<sup>51</sup> were used in the calculations with the following valence electron configuration:  $3s^2 3p^6 4s^2$  (Sr),  $4s^2 4p^6 5s^2$  (Ba),  $4s^2 4p^6 5s^2 4d^1$  (Y),  $6s^2 6p^3$  (Bi),  $3p^6 4s^2 3d^2$  (Ti),  $3p^6 4s^2 3d^5$  (Mn),  $3p^6 4s^2 3d^6$  (Fe) and  $2s^2 2p^4$  (O). Spontaneous polarizations were computed using the Berry-phase approach and phonons and Born effective charges were computed using the density functional perturbation theory<sup>52</sup>. The electric field effect was modelled using a linear response approach by freezing-in some lattice distortion into the system<sup>53,54</sup>. Symmetry mode analyses were performed using the Amplimodes software from the Bilbao Crystallographic server<sup>55,56</sup>.

## ACKNOWLEDGMENTS

Work supported by the ARC project TheMoTherm and F.R.S-FNRS PDR project HiT4FiT. Ph. Ghosez acknowledges the Francqui Foundation and N.C. Bristowe the Royal Commission of the Exhibition of 1851 for a fellowship at Imperial College London. Calculations have been performed within the PRACE projects TheoMoMuLaM and TheDeNoMo. They also took advantage of the Céci facilities funded by F.R.S-FNRS (Grant No 2.5020.1) and Tier-1 supercomputer of the Fédération Wallonie-Bruxelles funded by the Walloon Region (Grant No 1117545).

\* These two authors contributed equally

- <sup>1</sup> P. Zubko, S. Gariglio, M. Gabay, P. Ghosez, and J.-M. Triscone, *Annu. Rev. Condens. Matter Phys.* **2**, 141 (2011).
- <sup>2</sup> H. Köppel, D. R. Yarkony, and H. Barentzen, *The Jahn-Teller Effect* (Springer, 2009).
- <sup>3</sup> J. Goodenough, *Annual review of materials science* **28**, 1 (1998).
- <sup>4</sup> B. Raveau, M. Hervieu, A. Maignan, and C. Martin, *J. Mater. Chem.* **11**, 29 (2001).
- <sup>5</sup> J. G. Bednorz and K. A. Müller, *Rev. Mod. Phys.* **60**, 585 (1988).
- <sup>6</sup> J. Han, O. Gunnarsson, and V. Crespi, *Phys. Rev. Lett.* **90**, 167006 (2003).
- <sup>7</sup> R. Berthelot, D. Carlier, and C. Delmas, *Nature Materials* **10**, 74 (2011).
- <sup>8</sup> A. Glazer, *Acta Cryst. B* **28**, 3384 (1972).
- <sup>9</sup> N.A. Benedek and C. J. Fennie, *J. Phys. Chem. C* **117**, 13339 (2013).

- <sup>10</sup> E. Bousquet, M. Dawber, N. Stucki, C. Lechtensteiger, P. Hermet, S. Gariglio, J. M. Gariglio, and P. Ghosez, *Nature* **452**, 732 (2008).
- <sup>11</sup> T. Fukushima, A. Stroppa, S. Picozzi, and J. M. Perez-Mato, *Phys. Chem. Chem. Phys.* **13**, 12186 (2011).
- <sup>12</sup> J. M. Rondinelli and C. J. Fennie, *Adv. Materials* **24**, 1961 (2012).
- <sup>13</sup> J. Varignon, N. C. Bristowe, E. Bousquet, and P. Ghosez, *Comptes Rendus Physique* **16**, 153 (2015).
- <sup>14</sup> Z. Zanolli, J. C. Wojdel, J. Iñiguez, and P. Ghosez, *Phys. Rev. B* **88**, 060102(R) (2013).
- <sup>15</sup> A. Stroppa, P. Barone, P. Jain, J. M. Perez-Mato, and S. Picozzi, *Adv. Mater.* **25**, 2284 (2013).
- <sup>16</sup> Y. Tian, A. Stroppa, Y.-S. Chai, P. Barone, M. Perez-Mato, S. Picozzi, and Y. Sun, *Physica Status Solidi (RRL)* (2014).
- <sup>17</sup> N. A. Benedek and C. J. Fennie, *Phys. Rev. Lett.* **106**, 107204 (2011).



- <sup>18</sup> N. A. Benedek, A. T. Mulder, and C. J. Fennie, *J. Solid State Chem.* **195**, 11 (2012).
- <sup>19</sup> J. Varignon, N. C. Bristowe, E. Bousquet, and P. Ghosez, (2014), arXiv preprint arXiv:1409.8422.
- <sup>20</sup> N. C. Bristowe, J. Varignon, D. Fontaine, E. Bousquet, and P. Ghosez, *Nat. Commun.* **6**, 6677 (2015).
- <sup>21</sup> N. Miao, N. C. Bristowe, B. Xu, M. J. Verstraete, and P. Ghosez, *J. Phys.: Cond. Matt.* **26**, 035401 (2014).
- <sup>22</sup> P. V. Balachandran and J. M. Rondinelli, *Phys. Rev. B* **88**, 054101 (2013).
- <sup>23</sup> N. A. Benedek, J. M. Rondinelli, H. Djani, Ph. Ghosez and PH. Lightfoot, *Dalton Transactions* (2015).
- <sup>24</sup> Being in the  $Pb2_1m$  phase is sufficient but *a priori* not mandatory to achieve our goal. From eq 1, only the coupling between the polar and JT distortions is key to achieve an electric field control of the Jahn-Teller distortions. Indeed, one can imagine a metastable phase only developing the antipolar A distortion. Applying an electric field would activate the polar mode and through the first term of eq. 1, the Jahn-Teller distortion may automatically appear. However, in practice this metastable phase does not seem to be favoured, and being in the ground state ferroelectric phase may bring added functionality such as switchable behaviour.
- <sup>25</sup> M. A. Carpenter and C. J. Howard, *Acta Cryst. B* **65**, 134 (2009).
- <sup>26</sup> Y. Yang, W. Ren, M. Stengel, X. Yan, and L. Bellaiche, *Physical Rev. Lett.* **109**, 057602 (2012).
- <sup>27</sup> Y. Yang, J. Íñiguez, A.-J. Mao, and L. Bellaiche, *Phys. Rev. Lett.* **112**, 057202 (2014).
- <sup>28</sup> Q. Zhou and K. M. Rabe, arXiv preprint arXiv:1306.1839 (2013).
- <sup>29</sup> D. M. Hatch and H. T. Stokes, *J. Applied Cryst.* **36**, 951 (2003).
- <sup>30</sup> J. H. Haeni, P. Irvin, W. Chang, R. Uecker, P. Reiche, Y. L. Li, S. Choudhury, W. Tian, M. E. Hawley, B. Craigo, A. K. Tagantsev, X. Q. Pan, S. K. Streiffer, L. Q. Chen, S. W. Kirchoefer, J. Levy, and D. G. Schlom, *Nature* **430**, 758 (2004).
- <sup>31</sup> J. Junquera and P. Ghosez, *J. Comput. Theo. Nanosci.* **5**, 2071 (2008).
- <sup>32</sup> S. Bhattacharjee, E. Bousquet, and P. Ghosez, *Phys. Rev. Lett.* **102**, 117602 (2009).
- <sup>33</sup> T. Günter, E. Bousquet, A. David, P. Boullay, P. Ghosez, W. Prellier, and M. Fiebig, *Phys. Rev. B* **85**, 214120 (2012).
- <sup>34</sup> C. J. Fennie and K. M. Rabe, *Phys. Rev. Lett.* **97**, 267602 (2006).
- <sup>35</sup> J. H. Lee, L. Fang, E. Vlahos, X. Ke, Y. W. Jung, L. F. Kourkoutis, J.-W. Kim, P. J. Ryan, T. Heeg, M. Roederath, V. Goian, M. Bernhagen, R. Uecker, P. C. Hammel, K. M. Rabe, S. Kamba, J. Schubert, J. W. Freeland, D. A. M. C. J. Fennie and P. Schiffer, V. Gopalan, E. Johnston-Halperin, and D. G. Schlom, *Nature* **466**, 954 (2010).
- <sup>36</sup> Z. Fan, J. Wang, M. B. Sullivan, A. Huan, D. J. Singh, and K. P. Ong, *Scientific Reports* **4** (2014).
- <sup>37</sup> Y. Hou, J. Yang, X. Gong, and H. Xiang, *Physical Rev. B* **88**, 060406 (2013).
- <sup>38</sup> While the ground state of  $BaMnO_3$  has been shown to adopt a hexagonal polar  $P63cm$  structure<sup>46</sup>,  $BaMnO_3$  can also be stabilized with a perovskite form under tensile strain<sup>42</sup>.
- <sup>39</sup> The strain percentage is defined as the elongation with respect to the  $\sqrt{2}a, \sqrt{2}b$  axes of the pseudo cubic structure corresponding to the fully relaxed ground state. The fully relaxed ground states for all compounds are given in the supplementary materials.
- <sup>40</sup> We only report in table I the relevant distortions for the proposed mechanism. One should notice that due to a small tolerance factor,  $BiFeO_3$  and  $YMnO_3$  still develop large  $aa^-c^0$  rotations in their ground state, in addition to other antipolar modes. Their  $Pb2_1m$  phase may appear to be derived from a  $R3c$  or  $Pbnm$  structure respectively.
- <sup>41</sup> J. H. Lee, K. T. Delaney, E. Bousquet, N. A. Spaldin, and K. M. Rabe, *Physical Rev. B* **88**, 174426 (2013).
- <sup>42</sup> J. M. Rondinelli, A. S. Eidelson, and N. A. Spaldin, *Phys. Rev. B* **79**, 205119 (2009).
- <sup>43</sup> The JT distortion in  $YMnO_3$  appears through an electronic instability mechanism in the high symmetry phase. Indeed, only removing the symmetry on the electronic wavefunction while keeping the centrosymmetric positions for the cations produces already an energy gain, that is then amplified by the resulting JT lattice distortions.
- <sup>44</sup> In reference 27, authors report a relatively weak polar instability in the  $P4/mmm$  phase that we do not obtain in our simulations. This contradiction may be related to technical details or the magnitude of the strain applied, but in any case will not affect the final result of the present letter.
- <sup>45</sup> The two average ab-plane Mn-O bond lengths are evaluated to be  $\langle d_{MnO} \rangle_{ab,1} = 1.903 \text{ \AA}$  and  $\langle d_{MnO} \rangle_{ab,2} = 2.438 \text{ \AA}$  while the average Mn-O bond length along the c axis is around  $\langle d_{MnO} \rangle_c = 1.900 \text{ \AA}$ . Consequently, the  $d_{x^2y^2}$  orbital should be more stable than the  $d_{z^2}$  orbital. Considering the sole  $Q_2^+$  distortion, the two in-plane Mn-O bond lengths are 2.294  $\text{\AA}$  and 1.772  $\text{\AA}$  while the out of plane bond length is 1.769  $\text{\AA}$ .
- <sup>46</sup> J. Varignon and P. Ghosez, *Phys. Rev. B* **87**, 140403(R) (2013).
- <sup>47</sup> G. Kresse and J. Haffner, *Phys. Rev. B* **47**, 558 (1993).
- <sup>48</sup> G. Kresse and J. Furthmüller, *Computational Materials Science* **6**, 15 (1996).
- <sup>49</sup> J. P. Perdew, A. Ruzsinszky, G. I. Csonka, O. A. Vydrov, G. E. Scuseria, L. A. Constantin, X. Zhou, and K. Burke, *Phys. Rev. Lett.* **100**, 136406 (2008).
- <sup>50</sup> A. I. Liechtenstein, V. I. Anisimov, and J. Zaanen, *Phys. Rev. B* **52**, R5467 (1995).
- <sup>51</sup> P. E. Blöchl, *Physical Review B* **50**, 17953 (1994).
- <sup>52</sup> S. Baroni, S. de Gironcoli, A. Dal Corso, and P. Giannozzi, *Rev. Mod. Phys.* **73**, 515 (2001).
- <sup>53</sup> J. Íñiguez, *Phys. Rev. Lett.* **101**, 117201 (2008).
- <sup>54</sup> J. Varignon, S. Petit, A. Gellé, and M. B. Lepetit, *J. Phys.: Condens. Matt.* **25**, 496004 (2013).
- <sup>55</sup> D. Orobengoa, C. Capillas, M. I. Aroyo, and J. M. Perez-Mato, *J. App. Cryst.* **42**, 820 (2009).
- <sup>56</sup> J. Perez-Mato, D. Orobengoa, and M. Aroyo, *Acta Cryst. A* **66**, 558 (2010).